

Supplemental Material

1. Derivation of the 2T expression for \bar{v}_r from the Wannier equation. We begin by dividing the Wannier expression, eq 6, by $m/2$.

$$\frac{1}{2}m\bar{v}^2 \approx \frac{3}{2}kT + \frac{1}{2}mv_d^2 + \frac{1}{2}Mv_d^2 \quad (\text{S1})$$

$$\bar{v}^2 = \frac{3kT}{m} + \frac{v_d^2}{\hat{m}} \quad (\text{S2})$$

Using the definition of relative velocity, $v_r \equiv v - V$, it is possible to eliminate \bar{v}^2 in favor of \bar{v}_r^2 , because the average of $v \cdot V$ over all collisions vanishes.

$$\bar{v}_r^2 = \bar{v}^2 + \bar{V}^2 - 2\bar{v} \cdot \bar{V} = \bar{v}^2 + \bar{V}^2 = \bar{v}^2 + \frac{3kT}{M} \quad (\text{S3})$$

Substituting S3 into S2,

$$\bar{v}_r^2 = \frac{3kT}{m} + \frac{3kT}{M} + \frac{v_d^2}{\hat{m}} = \frac{3kT}{\mu} + \frac{v_d^2}{\hat{m}} \quad (\text{S4})$$

We now assume that v_r has an MB distribution, so that we can write $\bar{v}_r = (8\bar{v}_r^2/3\pi)^{1/2}$.

$$\bar{v}_r^2 = \frac{8kT}{\pi\mu} + \frac{8}{3\pi\hat{m}}v_d^2 = v_T^2 + \frac{8}{3\pi\hat{m}}v_d^2 \quad (\text{S5})$$

Finally we factor out v_T^2 and take the square root.

$$\bar{v}_r = v_T \left(1 + \frac{8}{3\pi\hat{m}} \left(\frac{v_d}{v_T} \right)^2 \right)^{1/2} \quad (\text{S6})$$

We now have an expression to substitute into eq 5 for average relative speed, an expression that becomes v_T at very low field and $\left(\frac{8}{3\pi\hat{m}}\right)^{1/2}v_d$ at very high field.

2. Computation of \hat{c} and \hbar by numerical integration of $F(v_r)$. A collision between an ion with velocity v and a neutral with velocity V is conveniently described in terms of the relative velocity, $v_r \equiv v - V$, and the center-of-mass velocity, $v_{cm} \equiv \hat{m}v + MV$, for the pair. It is straightforward to show that a collision transfers energy from the ion to the neutral if and only if $v_r \cdot v_{cm} > 0$,

although the situation is complicated because energy is freely transferred among the three independent coordinate directions. For example, it is possible for an ion to lose energy in a collision where it gains z -momentum. Nevertheless, the preferred direction of ion motion, along the z -axis defined by the external electric field, E , allows an unambiguous classification of collisions on the basis of removing or adding energy in the ion's z -direction of motion, which we call "cooling" and "heating" classes of collisions, respectively. Note that in Reference 8 the cooling and heating definitions were based the sign of $v_r \cdot v_{cm}$, while we are now basing the definition on the sign of $v_{r,z}v_{cm,z}$.

Collisions may further be described as "r+" or "r-" depending on the sign of $v_r \cdot E$, and "cm+" or "cm-" depending on the sign of $v_{cm} \cdot E$, and thus divided into four [$r \pm, cm \pm$] classes based on the signs of $v_r \cdot E$ and $v_{cm} \cdot E$, in this order. The [+,-] and [-,-] classes comprise the cooling collisions, while the [+,-] and [-,+] classes comprise the heating collisions. We then may write $\hat{c} = [+^{\hat{+}}, +] + [-^{\hat{-}}, -]$ and $\hat{h} = [+^{\hat{+}}, -] + [-^{\hat{-}}, +]$, again using the "hat" notation to denote a fraction of some total, in this case fractions of the total number of collisions. At zero field $[+^{\hat{+}}, +] = [-^{\hat{-}}, -] = [+^{\hat{+}}, -] = [-^{\hat{-}}, +] = 0.25$, but at all field strengths above zero $[+^{\hat{+}}, +]$ increases while the other three fractions diminish. At every field strength $\hat{c} + \hat{h} = [+^{\hat{+}}, +] + [-^{\hat{-}}, -] + [+^{\hat{+}}, -] + [-^{\hat{-}}, +] = 1$.

Our strategy for estimating \hat{c} and \hat{h} is to construct the z -component of the relative velocity distribution, $F(v_r)$, from the z -components of the ion and neutral velocity distributions, $f(v)$ and $F(V)$, respectively. In Figure S1, $F(V)$ has been assumed to be a thermal (Maxwellian) distribution centered at zero velocity, while $f(v)$ has been assumed to be a thermal distribution centered at the average velocity of the ion swarm, i.e., $(v_x, v_y, v_z) = (0, 0, v_d)$. The numerical values in Figure S1 have been calculated for $m = 400$ g/mole, $M = 40$ g/mole, $K_0 = 20.0$ $\text{cm}^2\text{V}^{-1}\text{s}^{-1}$, $T = 300$ K, $P = 5$ torr, and $E/N = 1.55$ Td, a case chosen to make v_d equal to 20% of v_T . The horizontal axes in Figure S1 give velocity in units of v_T . Because $f(v)$ is an estimate, of course the $F(v_r)$ to be constructed will also be an estimate, as will be the values of \hat{c} and the momentum transfer coefficient.

From the definition of v_r and because $F(-V) = F(V)$, it may be shown that $F = f * F$, where "*" represents the convolution operation. For $v_r > 0$ the computation of F may be analyzed into components associated with $[+^{\hat{+}}, +]$ and $[+^{\hat{+}}, -]$ using eq S7.

$$F(v_r) = \int_{-\infty}^{\infty} f(v)F(v + v_r)dv = \quad (S7)$$

$$\int_{-\infty}^{\hat{M}\nu_r} f(v)F(v + \nu_r)dv + \int_{\hat{M}\nu_r}^{\infty} f(v)F(v + \nu_r)dv \equiv F_{+-} + F_{++}$$

Figure S1.A shows explicitly, for the experimental condition $\nu_d = 0.2\nu_T$, how one value, $F(\nu_r = 1)$, is calculated by shifting F by 1, followed by multiplication of corresponding values of f and F , and integrating. The split point of the integral at $v = \hat{M}\nu_r$, shown as the vertical $\nu_{cm} = 0$ line in Figure 1.A, corresponds to collisions which neither heat nor cool the ion, i.e., in which the ion's z -velocity simply changes sign and there is no energy gain or loss. Cooling collisions lie to the right of the line, and heating collisions to the left. Equation S7 also works for $\nu_r < 0$, except the first integral in the second line becomes the expression for F_{--} and the second for F_{-+} .

The $F(\nu_r)$ produced by this construction is shown in Figure S1.B, along with its decomposition into the F_{++} , F_{+-} , F_{--} , and F_{-+} components. The $\nu_r = 0$ line in Figure S1.B corresponds to ions and neutrals moving with the same velocity, which means that they cannot collide. The jaggedness of the lines in Figure S1.B arises because the integrations of eq S7 have been performed numerically on a $\Delta\nu_r = 0.1\nu_T$ grid.

The value $F(\nu_r)$ is the probability of finding an ion with this particular ν_r , so the probability of a collision at this relative velocity is given by $|\nu_r|F(\nu_r)$, as shown in Figure S1.C. The fractions of cooling and heating collisions are then given by eq S8.

$$\hat{c} = \frac{\int (F_{++} + F_{--})v dv}{\int (F_{++} + F_{+-} + F_{-+} + F_{--})v dv} = 1 - \hat{h} \quad (\text{S8})$$

Numerical integration of eq S8 gives $\hat{c} = 0.6922$ for the case of the experimental condition $\nu_d = 0.2\nu_T$ illustrated in Figure S1. When this calculation of \hat{c} is repeated for a range of ν_d/ν_T the result is Figure 2. A tabulation of the computed values is given in Table S1. By using Figure 2 or interpolation using values from Table S1, a value of α can be obtained using eq 14 with any experimental values of m , M , ν_d , and ν_T .

Fig. S1.A includes cartoons of archetype collisions for the four $[r \pm, cm \pm]$ classes, using larger red circles to represent m , smaller blue circles for M , and arrows to represent motion in the laboratory frame of reference. Note that by adding the same amount of velocity to both m and M the $[+, +]$ and $[-, +]$ classes can be transformed into one another, as can the $[+, -]$ and $[-, -]$ classes, whereas $m \leftrightarrow M$ exchange leads to the interchanges $[+, +] \leftrightarrow [+, -]$ and $[-, +] \leftrightarrow [-, -]$. An alternate analysis to eq S8 would be to take $\hat{c} \equiv [+, +] - [-, +]$ and $\hat{h} \equiv [+, -] - [-, -]$. At very

low fields this analysis leads to the same values of \hat{c} and \hat{h} as eq S8, but at higher fields leads to greater cooling-heating divergence and poorer agreement with accurately computed hard-sphere mobilities in comparison to eq S8. This analysis inspires the discussion of cooling and heating given in the main text, organized around Fig. 1 and the counterfactual assignment of charge to the neutrals when accounting for the effect of heating collisions on the momentum-transfer coefficient.

3. Computation of \bar{v}_r by numerical integration. To compute the average length of the vector

sum of an ion velocity of magnitude $\frac{\beta}{\alpha}v_d$, oriented as in Figure 3.B or 3.D, with the arbitrarily oriented vector v_T , assume that angle between the two vectors is $0 \leq \omega \leq \pi$. The sum of the two vectors, v_s , is given by eq S9.

$$v_s = \left(\frac{\beta}{\alpha} v_d, 0 \right) + (v_T \cos \omega, v_T \sin \omega) = \left(\frac{\beta}{\alpha} v_d + v_T \cos \omega, v_T \sin \omega \right) \quad (\text{S9})$$

The length of v_s is then given by eq S10.

$$v_s = \left[\left(\frac{\beta}{\alpha} v_d + v_T \cos \omega \right)^2 + v_T^2 (\sin \omega)^2 \right]^{1/2} = \left[v_T^2 + \left(\frac{\beta}{\alpha} \right)^2 v_d^2 + \frac{2\beta}{\alpha} v_d v_T \cos \omega \right]^{1/2} \quad (\text{S10})$$

Since v_s can have any azimuth orientation, $0 \leq \rho \leq 2\pi$, its overall contribution to \bar{v}_r should have the weight $2\pi v_T \sin \omega$, and \bar{v}_r is given by eq S11.

$$\bar{v}_r = \frac{2\pi v_T \int_0^\pi v_s \sin \omega d\omega}{2\pi v_T \int_0^\pi \sin \omega d\omega} \quad (\text{S11})$$

If the $\cos \omega$ term inside the square bracket of eq S10 is ignored, eq S11 leads immediately to eq 23. Carrying out numerical integration of eq S11 with an 1800 bin grid leads to the values given

in Table S3 for a range of $\frac{\beta}{\alpha} v_d$ to v_T ratios. This Table also contains the approximate values from eq 23 and their relative errors. Finally the errors from Table S3 are plotted in Fig. S2.

v_d/v_T	\hat{c}	v_d/v_T	\hat{c}	v_d/v_T	\hat{c}	v_d/v_T	\hat{c}
0.00	0.5000	0.40	0.8359	0.80	0.9662	1.20	0.9951
0.01	0.5115	0.41	0.8415	0.81	0.9677	1.21	0.9953
0.02	0.5215	0.42	0.8469	0.82	0.9691	1.22	0.9956
0.03	0.5315	0.43	0.8522	0.83	0.9704	1.23	0.9958
0.04	0.5415	0.44	0.8574	0.84	0.9717	1.24	0.9960
0.05	0.5515	0.45	0.8624	0.85	0.9729	1.25	0.9962
0.06	0.5614	0.46	0.8673	0.86	0.9741	1.26	0.9964
0.07	0.5712	0.47	0.8721	0.87	0.9753	1.27	0.9966
0.08	0.5810	0.48	0.8767	0.88	0.9763	1.28	0.9968
0.09	0.5908	0.49	0.8811	0.89	0.9774	1.29	0.9970
0.10	0.6004	0.50	0.8855	0.90	0.9784	1.30	0.9971
0.11	0.6100	0.51	0.8897	0.91	0.9794	1.31	0.9973
0.12	0.6196	0.52	0.8938	0.92	0.9803	1.32	0.9974
0.13	0.6290	0.53	0.8977	0.93	0.9812	1.33	0.9976
0.14	0.6384	0.54	0.9015	0.94	0.9821	1.34	0.9977
0.15	0.6476	0.55	0.9052	0.95	0.9829	1.35	0.9978
0.16	0.6567	0.56	0.9088	0.96	0.9837	1.36	0.9980
0.17	0.6658	0.57	0.9123	0.97	0.9844	1.37	0.9981
0.18	0.6747	0.58	0.9157	0.98	0.9851	1.38	0.9982
0.19	0.6835	0.59	0.9189	0.99	0.9858	1.39	0.9983
0.20	0.6922	0.60	0.9221	1.00	0.9865	1.40	0.9984
0.21	0.7007	0.61	0.9251	1.01	0.9871	1.41	0.9985
0.22	0.7092	0.62	0.9280	1.02	0.9877	1.42	0.9986
0.23	0.7174	0.63	0.9309	1.03	0.9883	1.43	0.9987
0.24	0.7256	0.64	0.9336	1.04	0.9889	1.44	0.9988
0.25	0.7336	0.65	0.9363	1.05	0.9894	1.45	0.9988
0.26	0.7415	0.66	0.9388	1.06	0.9899	1.46	0.9989
0.27	0.7492	0.67	0.9413	1.07	0.9904	1.47	0.9990
0.28	0.7568	0.68	0.9437	1.08	0.9909	1.48	0.9990
0.29	0.7642	0.69	0.9459	1.09	0.9913	1.49	0.9991
0.30	0.7715	0.70	0.9481	1.10	0.9917	1.50	0.9992
0.31	0.7786	0.71	0.9503	1.11	0.9921		
0.32	0.7856	0.72	0.9523	1.12	0.9925		
0.33	0.7924	0.73	0.9543	1.13	0.9929		
0.34	0.7991	0.74	0.9562	1.14	0.9932		
0.35	0.8056	0.75	0.9580	1.15	0.9936		
0.36	0.8119	0.76	0.9598	1.16	0.9939		
0.37	0.8181	0.77	0.9615	1.17	0.9942		
0.38	0.8242	0.78	0.9631	1.18	0.9945		
0.39	0.8301	0.79	0.9647	1.19	0.9948		

Table S1. Fraction of cooling collisions at various v_d/v_T values

<i>m</i> (g/mole)	<i>M</i> (g/mole)	Accuracy
20.2	2020	0.5%
22	220	0.04% below and 0.5% above 5 Td
40	40	0.04%
220	22	0.04% below 364 Td, 0.5% for 364-719 Td, 2% above 719 Td
2020	20.2	0.04%

Table S2. Input masses and accuracies of the calculated mobilities

$v_0 = \beta v_d / \alpha$	v_T	$(v_0^2 + v_T^2)^{1/2}$	\bar{v}_r from eq S11	Rel. Err. in \bar{v}_r
0.01	1.00	1.0000	1.0000	0.0000
0.10	1.00	1.0050	1.0033	0.0016
0.20	1.00	1.0198	1.0133	0.0064
0.30	1.00	1.0440	1.0300	0.0136
0.40	1.00	1.0770	1.0533	0.0225
0.50	1.00	1.1180	1.0833	0.0320
0.60	1.00	1.1662	1.1200	0.0412
0.70	1.00	1.2207	1.1633	0.0493
0.80	1.00	1.2806	1.2133	0.0555
0.90	1.00	1.3454	1.2700	0.0593
1.00	1.00	1.4142	1.3333	0.0607
1.10	1.00	1.4866	1.4030	0.0596
1.20	1.00	1.5620	1.4778	0.0570
1.30	1.00	1.6401	1.5564	0.0538
1.40	1.00	1.7205	1.6381	0.0503
1.50	1.00	1.8028	1.7222	0.0468
1.60	1.00	1.8868	1.8083	0.0434
1.70	1.00	1.9723	1.8961	0.0402
1.80	1.00	2.0591	1.9852	0.0372
1.90	1.00	2.1471	2.0754	0.0345
2.00	1.00	2.2361	2.1667	0.0320
2.50	1.00	2.6926	2.6333	0.0225
3.33	1.00	3.4801	3.4333	0.0136
5.00	1.00	5.0990	5.0667	0.0064
10.00	1.00	10.0499	10.0333	0.0016
100.00	1.00	100.0050	100.0033	

Table S3. Average relative speed computed by eq 23 and by numerical integration of eq S11. The relative errors are plotted in Fig. S2.

E/N	K ₀	E/N	K ₀	E/N	K ₀	E/N	K ₀	E/N	K ₀
0.01	2.390	55.47	2.202	164.72	1.705	629.21	0.986	2873.1	0.477
0.03	2.390	56.75	2.196	169.72	1.688	652.63	0.970	2987.1	0.468
0.12	2.390	60.82	2.174	174.91	1.671	677.01	0.953	3105.7	0.459
0.50	2.390	62.26	2.166	180.20	1.654	702.36	0.937	3229.1	0.450
1.98	2.389	63.74	2.159	185.87	1.636	728.73	0.922	3357.5	0.442
3.47	2.389	65.26	2.151	191.67	1.618	756.17	0.906	3491.4	0.433
4.86	2.388	66.82	2.142	197.69	1.600	784.71	0.890	3630.0	0.425
6.81	2.386	68.43	2.134	203.94	1.582	814.40	0.875	3774.6	0.417
8.17	2.384	70.09	2.125	210.43	1.564	845.28	0.860	3925.0	0.409
9.82	2.382	71.80	2.116	217.17	1.546	877.42	0.845	4081.5	0.401
11.80	2.379	73.56	2.106	224.17	1.527	910.84	0.830	4244.3	0.393
13.59	2.375	75.38	2.097	231.44	1.509	945.62	0.816	4413.7	0.386
15.66	2.371	77.25	2.087	238.99	1.491	981.80	0.801	4590.0	0.379
18.05	2.365	79.18	2.077	246.84	1.472	1019.4	0.787	4773.3	0.371
19.90	2.359	81.17	2.067	255.00	1.454	1058.5	0.773	4964.1	0.364
21.95	2.353	83.22	2.056	263.48	1.435	1099.3	0.760	5162.6	0.357
24.23	2.345	85.34	2.045	272.30	1.416	1141.7	0.746	5369.1	0.350
25.49	2.340	87.52	2.034	281.44	1.398	1185.7	0.733	5583.9	0.344
26.81	2.336	89.78	2.023	290.96	1.379	1231.6	0.719	5807.4	0.337
28.22	2.331	92.11	2.011	300.85	1.360	1279.3	0.706	6040.0	0.330
29.70	2.325	94.52	1.999	311.13	1.342	1329.0	0.694	6281.9	0.324
31.28	2.319	97.00	1.987	321.82	1.323	1380.6	0.681	6533.6	0.318
32.94	2.312	99.57	1.974	332.94	1.305	1434.4	0.669	6795.5	0.312
34.70	2.304	102.23	1.961	344.49	1.286	1490.3	0.656	7068.0	0.306
36.57	2.296	104.98	1.948	356.51	1.268	1548.4	0.644	7351.5	0.300
38.55	2.287	107.81	1.935	369.00	1.249	1608.9	0.633	7646.4	0.294
40.65	2.277	110.75	1.921	381.99	1.231	1671.9	0.621	7953.2	0.288
41.54	2.273	113.79	1.908	395.50	1.213	1737.4	0.610	8272.5	0.283
42.46	2.268	116.93	1.893	409.55	1.194	1805.5	0.598	8604.6	0.277
43.39	2.264	120.19	1.879	424.16	1.176	1876.4	0.587		
44.35	2.259	123.56	1.864	439.36	1.158	1950.2	0.576		
45.34	2.254	127.05	1.849	455.16	1.140	2026.9	0.566		
46.35	2.249	130.66	1.834	471.60	1.123	2106.7	0.555		
47.39	2.244	134.40	1.819	488.69	1.105	2189.8	0.545		
48.45	2.239	138.28	1.803	506.48	1.088	2276.2	0.534		
49.55	2.233	142.30	1.788	524.97	1.070	2366.1	0.524		
50.67	2.227	146.46	1.771	544.21	1.053	2459.6	0.515		
51.82	2.221	150.78	1.755	564.22	1.036	2556.9	0.505		
53.00	2.215	155.26	1.739	585.03	1.019	2658.2	0.495		
54.22	2.209	159.91	1.722	606.68	1.003	2763.5	0.486		

Table S4. K₀ (cm²V⁻¹s⁻¹) as a function of E/N (Td) for (m/M)=100

E/N	K ₀	E/N	K ₀	E/N	K ₀	E/N	K ₀	E/N	K ₀
0.01	2.391	53.56	2.193	156.47	1.702	597.85	0.988	3583.3	0.418
0.03	2.391	54.81	2.186	161.23	1.685	620.07	0.971	3722.9	0.411
0.12	2.391	56.10	2.179	166.17	1.668	643.19	0.955	3871.3	0.403
0.47	2.391	57.43	2.171	171.30	1.651	667.24	0.939	4025.5	0.395
1.90	2.390	58.79	2.163	176.63	1.633	692.26	0.923	4186.1	0.388
3.32	2.389	61.63	2.147	182.15	1.616	718.28	0.907	4353.4	0.380
4.66	2.389	63.13	2.139	187.88	1.598	746.00	0.891	4527.2	0.373
6.52	2.387	64.66	2.130	193.84	1.580	773.48	0.877	4708.1	0.366
7.83	2.385	66.24	2.121	200.02	1.562	802.77	0.862	4896.3	0.359
9.41	2.382	67.87	2.112	206.44	1.544	833.29	0.847	5092.0	0.352
11.31	2.379	69.54	2.103	213.10	1.526	865.00	0.832	5295.7	0.345
13.03	2.375	71.27	2.093	220.03	1.508	897.97	0.818	5507.6	0.338
15.01	2.370	73.05	2.084	227.22	1.489	932.28	0.804	5728.1	0.332
17.32	2.364	74.89	2.073	234.69	1.471	967.98	0.790	5957.5	0.325
19.09	2.358	76.79	2.063	242.45	1.452	1005.0	0.776	6196.1	0.319
21.07	2.351	78.74	2.052	250.52	1.434	1214.0	0.709	6444.4	0.313
23.26	2.343	80.76	2.041	258.90	1.415	1261.5	0.696	6962.2	0.301
24.48	2.338	82.84	2.030	267.60	1.397	1310.5	0.683	7251.0	0.295
25.76	2.333	84.99	2.019	276.65	1.378	1361.5	0.671	7542.0	0.290
27.11	2.328	87.21	2.007	286.06	1.360	1468.1	0.647	7844.7	0.284
28.54	2.322	89.51	1.995	295.84	1.342	1527.0	0.635	8159.6	0.278
30.06	2.315	91.88	1.983	306.00	1.323	1586.7	0.623	8487.2	0.273
31.67	2.308	94.33	1.970	316.56	1.305	1648.8	0.612		
33.37	2.299	96.86	1.958	327.54	1.287	1713.4	0.604		
35.20	2.289	99.48	1.945	338.96	1.268	1780.7	0.589		
37.10	2.281	102.19	1.931	350.83	1.249	1850.5	0.578		
39.14	2.271	104.99	1.918	363.17	1.231	1923.4	0.568		
40.01	2.266	107.89	1.904	376.26	1.212	1999.0	0.557		
40.89	2.262	110.89	1.890	389.35	1.194	2077.7	0.547		
41.80	2.257	113.99	1.875	403.22	1.176	2159.6	0.536		
42.74	2.252	117.21	1.861	417.65	1.159	2332.0	0.517		
43.69	2.247	120.53	1.846	432.66	1.141	2425.8	0.507		
44.68	2.242	123.98	1.831	448.27	1.123	2521.8	0.497		
45.69	2.236	127.55	1.816	464.48	1.106	2621.6	0.488		
46.72	2.231	131.25	1.800	481.42	1.089	2725.5	0.479		
47.79	2.225	135.08	1.784	498.94	1.072	2833.6	0.470		
48.88	2.219	139.06	1.768	517.19	1.055	2946.1	0.461		
50.00	2.213	143.18	1.752	536.18	1.038	3063.1	0.452		
51.16	2.206	147.45	1.736	555.93	1.021	3184.8	0.443		
52.34	2.200	151.87	1.719	576.48	1.004	3311.5	0.435		

Table S5. K₀ (cm²V⁻¹s⁻¹) as a function of E/N (Td) for (m/M)=10

E/N	K ₀	E/N	K ₀	E/N	K ₀	E/N	K ₀	E/N	K ₀
0.01	2.429	41.05	2.148	130.46	1.580	522.98	0.885	2421.1	0.424
0.02	2.429	41.98	2.143	134.65	1.562	542.80	0.870	2517.6	0.416
0.09	2.429	43.01	2.134	139.00	1.545	563.42	0.855	2617.9	0.408
0.35	2.429	44.07	2.125	143.52	1.527	584.87	0.840	2722.3	0.401
1.41	2.428	45.17	2.115	148.21	1.509	607.18	0.826	2830.9	0.393
2.47	2.427	46.30	2.105	153.09	1.491	630.39	0.812	2943.9	0.385
3.45	2.426	47.46	2.095	158.15	1.473	654.54	0.797	3061.4	0.378
4.84	2.422	48.66	2.085	163.42	1.454	679.65	0.783	3183.7	0.371
5.81	2.420	49.90	2.074	168.88	1.436	705.78	0.770	3310.9	0.364
6.99	2.416	51.18	2.064	174.56	1.418	732.96	0.756	3443.3	0.357
8.40	2.410	52.50	2.053	180.46	1.400	761.24	0.743	3581.1	0.350
9.69	2.404	53.86	2.042	186.61	1.381	790.66	0.730	3724.3	0.343
11.17	2.396	55.26	2.030	192.98	1.363	821.26	0.717	3873.4	0.337
12.89	2.386	56.72	2.018	199.61	1.346	853.10	0.704	4028.5	0.330
14.23	2.378	58.22	2.006	206.51	1.328	886.22	0.691	4189.9	0.324
15.72	2.368	59.77	1.994	213.67	1.310	920.68	0.679	4357.8	0.318
17.37	2.356	61.37	1.982	221.11	1.292	956.53	0.666	4532.4	0.311
18.30	2.349	63.03	1.969	228.85	1.274	993.86	0.654	4714.2	0.305
19.28	2.341	64.74	1.956	236.89	1.254	1032.6	0.642	4903.2	0.300
20.31	2.333	66.51	1.943	245.23	1.236	1073.0	0.631	5099.9	0.294
21.41	2.324	68.34	1.929	253.92	1.218	1115.0	0.619	5304.6	0.288
22.57	2.315	70.24	1.916	262.96	1.200	1158.7	0.608	5517.5	0.283
23.80	2.304	72.20	1.902	272.36	1.183	1204.1	0.596	5739.0	0.277
25.11	2.293	74.23	1.887	282.13	1.165	1251.4	0.585	5969.5	0.272
26.52	2.280	80.68	1.844	292.29	1.148	1300.6	0.575	6209.3	0.266
28.01	2.267	83.09	1.829	302.86	1.130	1351.8	0.564	6458.7	0.261
29.58	2.254	85.52	1.813	313.85	1.113	1405.1	0.554	6718.3	0.256
30.28	2.248	88.02	1.798	325.27	1.097	1460.5	0.543	6988.3	0.251
30.97	2.241	90.62	1.782	337.24	1.078	1518.1	0.533	7269.2	0.246
31.69	2.235	93.31	1.766	349.52	1.061	1578.1	0.523	7561.5	0.242
32.42	2.228	96.11	1.750	362.37	1.045	1640.5	0.513	7865.6	0.237
33.17	2.222	99.00	1.734	375.73	1.028	1705.4	0.504	8182.0	0.232
33.94	2.215	102.00	1.717	389.65	1.011	1772.9	0.494	8511.1	0.228
34.74	2.207	105.12	1.701	404.12	0.995	1843.1	0.485	8853.6	0.223
35.55	2.200	108.35	1.684	419.15	0.979	1916.2	0.476	9209.9	0.219
36.40	2.193	111.70	1.667	434.80	0.963	1992.3	0.467		
37.26	2.185	115.18	1.650	451.07	0.947	2071.4	0.458		
38.15	2.177	118.79	1.633	468.00	0.931	2153.7	0.449		
39.07	2.169	122.53	1.615	485.61	0.916	2239.3	0.441		
40.08	2.156	126.42	1.598	503.93	0.900	2328.4	0.433		

Table S6. K₀ (cm²V⁻¹s⁻¹) as a function of E/N (Td) for (m/M)=1

E/N	K ₀	E/N	K ₀	E/N	K ₀	E/N	K ₀	E/N	K ₀
0.02	2.609	19.18	2.146	63.18	1.456	279.84	0.751	1416.8	0.340
0.09	2.609	19.66	2.134	65.27	1.437	290.59	0.737	1473.4	0.334
0.38	2.609	20.16	2.121	67.43	1.418	301.77	0.724	1532.4	0.327
0.66	2.608	20.67	2.108	69.68	1.400	313.41	0.711	1593.7	0.321
1.15	2.605	21.20	2.094	72.03	1.381	325.51	0.698	1657.5	0.315
1.61	2.602	21.75	2.081	74.47	1.362	338.10	0.686	1723.9	0.309
2.26	2.595	22.31	2.067	77.00	1.343	351.20	0.673	1793.0	0.303
2.71	2.589	22.89	2.053	79.63	1.324	364.81	0.661	1864.8	0.297
3.26	2.580	23.49	2.039	82.36	1.306	378.98	0.649	1939.6	0.291
3.76	2.571	24.11	2.025	85.20	1.287	393.73	0.637	2017.4	0.286
4.34	2.559	24.75	2.011	88.15	1.269	409.07	0.626	2098.3	0.280
5.02	2.532	25.41	1.996	91.21	1.250	425.04	0.614	2182.5	0.275
5.78	2.516	26.09	1.980	94.39	1.232	441.64	0.603	2270.1	0.269
6.39	2.502	26.79	1.965	97.70	1.214	458.92	0.592	2361.2	0.264
7.06	2.485	27.52	1.950	101.14	1.196	476.89	0.581	2456.0	0.259
7.45	2.474	28.27	1.934	104.71	1.178	495.59	0.570	2554.7	0.254
7.85	2.464	29.04	1.918	108.43	1.160	515.05	0.560	2657.3	0.249
8.27	2.452	29.85	1.904	112.29	1.143	535.28	0.549	2764.1	0.244
8.72	2.440	30.69	1.891	116.31	1.125	556.34	0.539	2875.2	0.239
9.20	2.426	31.59	1.869	120.48	1.107	578.24	0.529	2990.7	0.235
9.70	2.412	32.44	1.853	124.81	1.090	601.03	0.519	3111.0	0.230
10.24	2.396	33.35	1.837	129.32	1.073	624.75	0.509	3236.1	0.226
10.80	2.386	34.32	1.820	134.03	1.056	649.41	0.500	3366.2	0.221
11.42	2.368	35.32	1.803	138.92	1.039	675.08	0.490	3501.7	0.217
12.06	2.348	36.35	1.785	144.01	1.022	701.78	0.481	3642.6	0.213
12.75	2.328	37.42	1.768	149.30	1.006	729.55	0.472	3789.1	0.209
13.10	2.318	38.54	1.751	154.81	0.989	758.46	0.463	3941.6	0.205
13.41	2.308	39.69	1.733	160.53	0.973	788.56	0.454	4100.3	0.201
13.73	2.299	40.88	1.715	166.48	0.957	819.85	0.446	4265.4	0.197
14.05	2.290	42.12	1.697	172.67	0.941	852.40	0.437	4437.1	0.193
14.38	2.280	43.41	1.679	179.10	0.925	886.26	0.429	4615.8	0.189
14.72	2.270	44.74	1.661	185.79	0.910	921.49	0.421	4801.7	0.185
15.07	2.260	46.12	1.642	192.76	0.894	958.14	0.413	4995.1	0.182
15.43	2.250	47.56	1.624	200.00	0.879	996.28	0.405	5196.3	0.178
15.80	2.239	49.05	1.605	207.54	0.864	1035.9	0.397	5405.3	0.175
16.18	2.228	50.59	1.587	215.37	0.849	1077.2	0.390	5623.1	0.171
16.57	2.217	52.19	1.568	223.53	0.835	1120.1	0.382	5849.7	0.168
16.98	2.206	53.86	1.549	232.01	0.820	1164.8	0.375	6085.4	0.165
17.39	2.194	55.58	1.531	240.84	0.806	1211.3	0.368		
17.82	2.183	57.38	1.512	250.01	0.792	1259.6	0.361		
18.26	2.171	59.24	1.493	259.58	0.778	1310.0	0.354		
18.71	2.159	61.17	1.474	269.51	0.764	1362.3	0.347		

Table S7. K₀ (cm²V⁻¹s⁻¹) as a function of E/N (Td) for (m/M)=0.1

E/N	K ₀	E/N	K ₀	E/N	K ₀	E/N	K ₀	E/N	K ₀
0.01	2.639	6.40	2.171	21.14	1.452	92.43	0.748	465.33	0.339
0.03	2.639	6.56	2.158	21.83	1.433	95.95	0.734	483.91	0.333
0.12	2.638	6.73	2.144	22.55	1.414	99.62	0.721	503.24	0.326
0.22	2.638	6.90	2.130	23.29	1.395	103.44	0.708	523.35	0.320
0.38	2.635	7.08	2.116	24.07	1.376	107.41	0.696	544.27	0.314
0.53	2.632	7.26	2.101	24.87	1.358	111.55	0.683	566.04	0.308
0.75	2.626	7.45	2.087	25.71	1.339	115.84	0.671	588.69	0.302
0.90	2.620	7.65	2.072	26.58	1.320	120.32	0.659	612.25	0.296
1.08	2.612	7.85	2.057	27.48	1.301	124.97	0.647	636.77	0.290
1.24	2.604	8.06	2.041	28.41	1.283	129.81	0.635	662.27	0.285
1.43	2.593	8.28	2.026	29.39	1.264	134.84	0.623	688.81	0.279
1.65	2.579	8.50	2.010	30.40	1.246	140.08	0.612	716.42	0.274
1.91	2.561	8.73	1.994	31.45	1.228	145.52	0.601	745.14	0.269
2.11	2.546	8.97	1.978	32.54	1.210	151.19	0.590	775.02	0.263
2.33	2.528	9.22	1.962	33.68	1.192	157.09	0.579	806.11	0.258
2.46	2.516	9.47	1.945	34.86	1.174	163.22	0.568	838.46	0.253
2.60	2.515	9.74	1.928	36.08	1.156	169.60	0.558	872.11	0.248
2.74	2.502	10.01	1.911	37.36	1.138	176.24	0.547	907.12	0.244
2.89	2.487	10.29	1.894	38.68	1.120	183.15	0.537	943.55	0.239
3.05	2.472	10.58	1.877	40.06	1.103	190.33	0.527	981.45	0.234
3.22	2.456	10.88	1.860	41.49	1.086	197.81	0.517	1020.8	0.230
3.39	2.438	11.20	1.842	42.98	1.069	205.59	0.508	1061.9	0.225
3.59	2.420	11.52	1.825	44.53	1.052	213.68	0.498	1104.5	0.221
3.79	2.400	11.85	1.807	46.13	1.035	222.10	0.489	1148.9	0.217
4.00	2.379	12.20	1.789	47.81	1.018	230.85	0.479	1195.1	0.212
4.23	2.356	12.56	1.771	49.55	1.002	239.96	0.470	1243.2	0.208
4.35	2.345	12.93	1.753	51.36	0.985	249.44	0.462	1293.2	0.204
4.46	2.335	13.32	1.734	53.24	0.969	259.30	0.453	1345.2	0.200
4.56	2.324	13.72	1.716	55.19	0.953	269.56	0.444	1399.4	0.196
4.67	2.314	14.13	1.697	57.23	0.937	280.24	0.436	1455.7	0.192
4.78	2.304	14.56	1.679	59.34	0.921	291.34	0.428	1514.3	0.189
4.90	2.295	15.00	1.660	61.54	0.906	302.90	0.420	1575.2	0.185
5.02	2.284	15.47	1.641	63.83	0.891	314.92	0.412	1638.6	0.181
5.14	2.273	15.94	1.623	66.21	0.875	327.42	0.404	1704.6	0.178
5.26	2.271	16.44	1.604	68.69	0.860	340.43	0.396	1773.3	0.174
5.39	2.259	16.95	1.585	71.26	0.846	353.97	0.388	1844.7	0.171
5.52	2.248	17.49	1.566	73.94	0.831	368.05	0.381	1919.0	0.168
5.65	2.236	18.04	1.547	76.73	0.817	382.70	0.374	1996.3	0.164
5.79	2.223	18.61	1.528	79.62	0.803	397.94	0.367		
5.94	2.211	19.21	1.509	82.64	0.789	413.80	0.360		
6.09	2.198	19.83	1.490	85.77	0.775	430.30	0.353		
6.24	2.185	20.47	1.471	89.03	0.761	447.47	0.346		

Table S8. K₀ (cm²V⁻¹s⁻¹) as a function of E/N (Td) for (m/M)=0.01

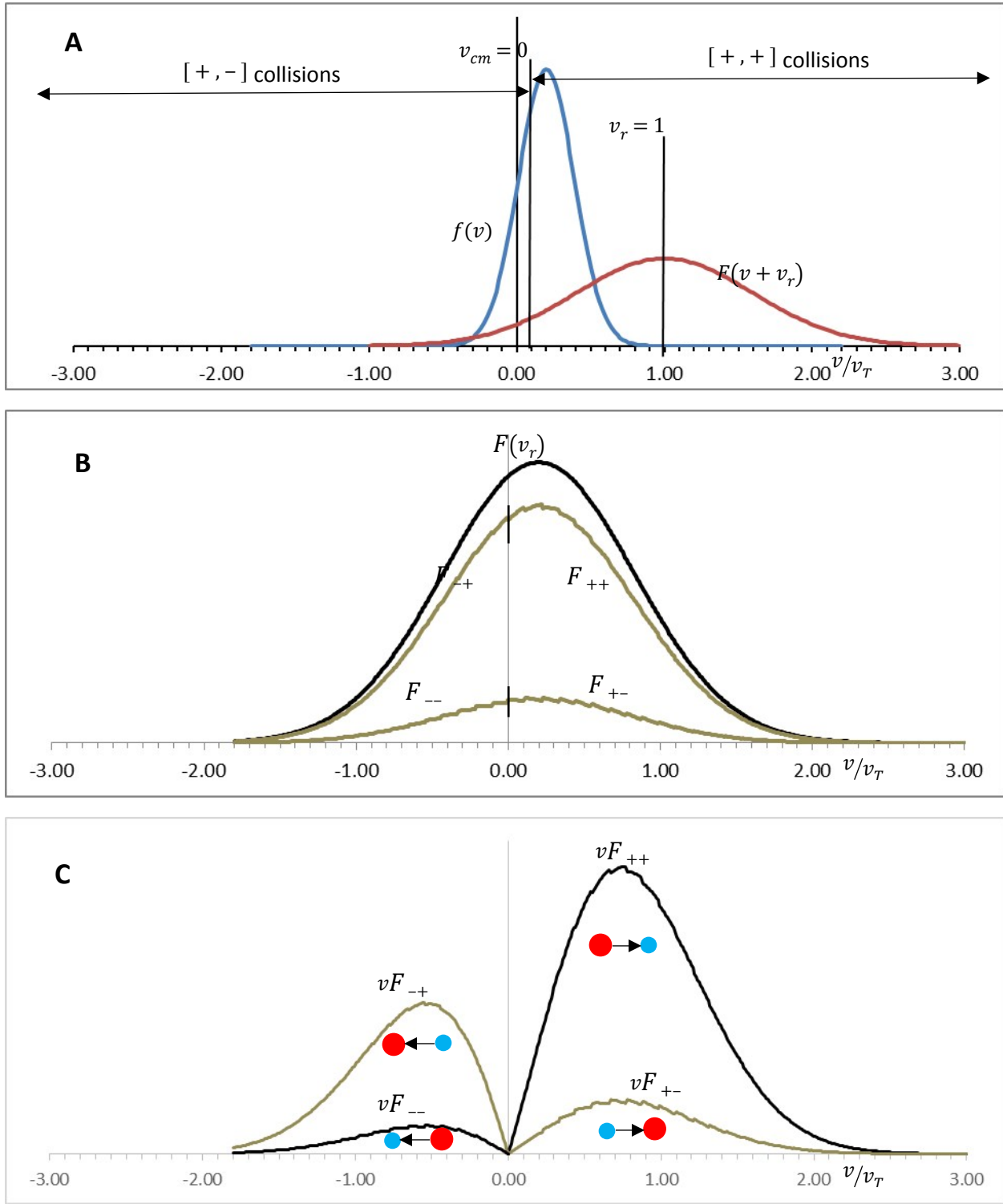


Figure S1. Estimation of relative velocity distribution and relative probabilities of cooling and heating collisions. A. The process for construction of $F(v_r) = f * F$, resolved into cooling and heating fractions, is illustrated for a single point, $v_r = 1.00 \times v_T$. B. The overall $F(v_r)$ is

shown resolved into its four disjoint components. C. Collision probabilities are shown for the four disjoint components of $F(v_r)$, cooling collisions by dark lines and heating collisions by light.

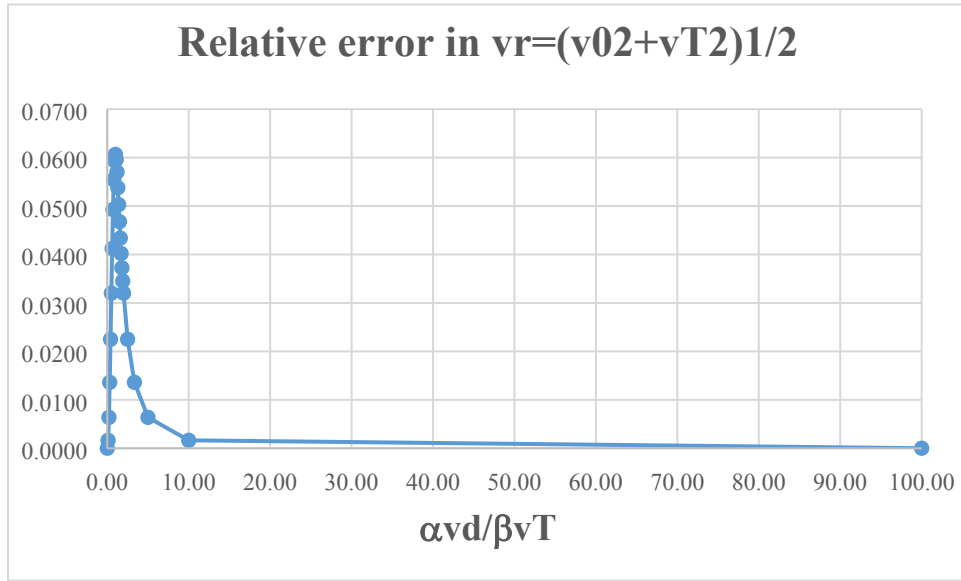


Figure S2. Relative error in $\bar{v}_r = \left[v_T^2 + \left(\frac{\alpha}{\beta} \right)^2 v_d^2 \right]^{1/2}$ compared to numerical integration of eq S11.

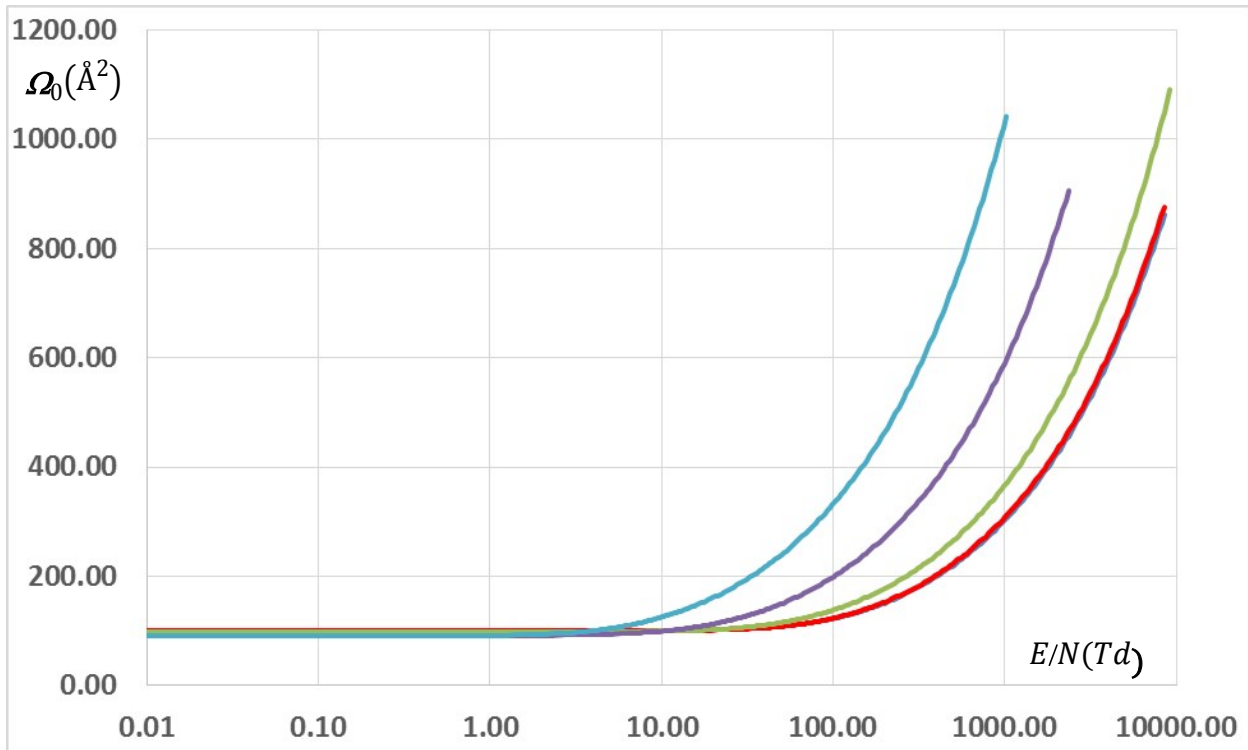


Figure S3. Zero-field cross sections calculated from the data of Fig. 4 using the eq 3. Expanded scale.

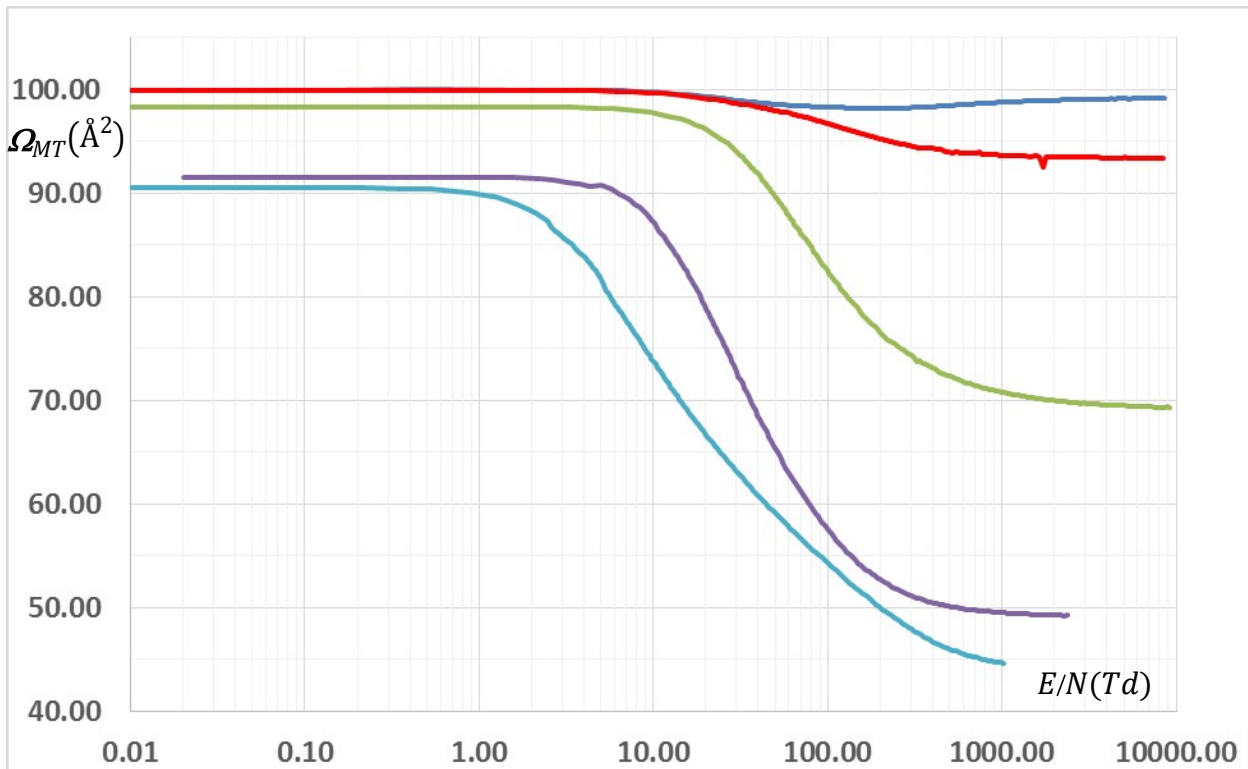


Figure S4. Momentum-transfer cross sections calculated from the data of Fig. 4 using eq 14. Expanded scale.

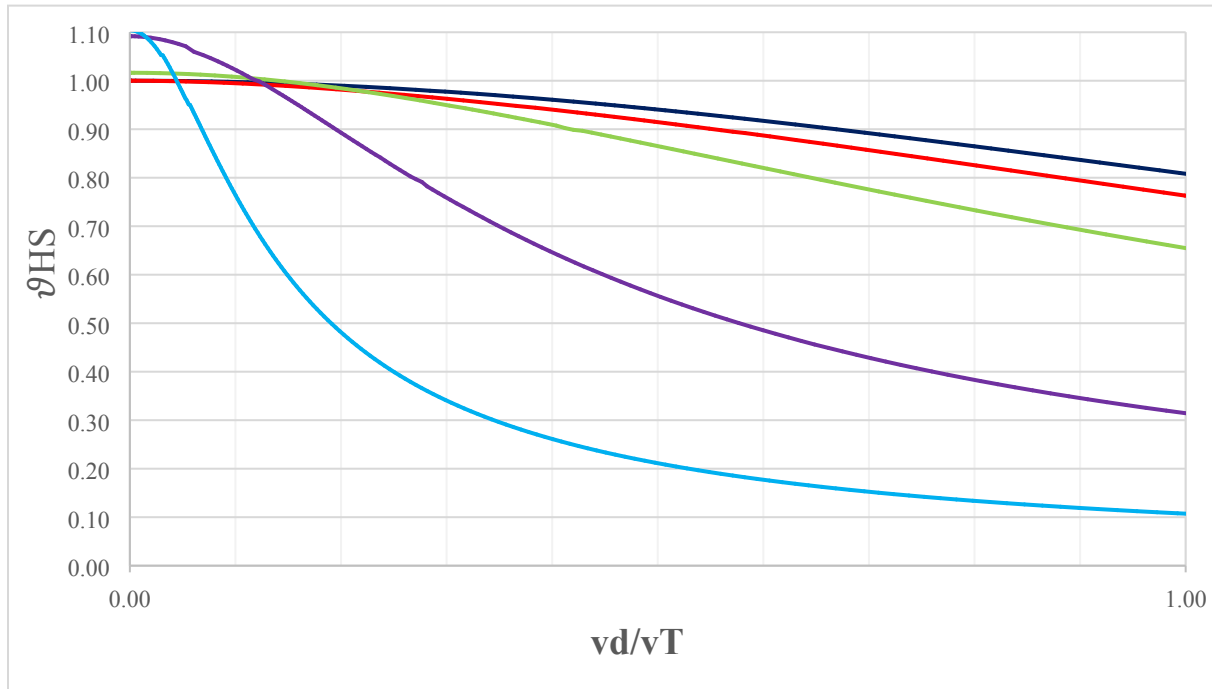


Figure S5. Hard sphere correction factor $\vartheta_{HS}\left(\frac{v_d}{v_T}\right)$ for use in eq 25. m/M values: 0.01 (light blue); 0.1 (purple); 1 (green); 10 (red); and 100 (dark blue).